Pflügers Arch (1984) 402:353–359

Pflügers Archiv
European Journal of Physiology

Effect of various cations and anions on the action of tetrodotoxin and saxitoxin on frog myelinated nerve fibers

S. Grissmer

I. Physiologisches Institut, Universität des Saarlandes, D-6650 Homburg/Saar, Federal Republic of Germany

Abstract. The influence of Mg^{2+}, La^{3+}, NO_3^-, and SCN^- on the equilibrium effect of tetrodotoxin (TTX) and saxitoxin (STX) on single myelinated nerve fibres of the frog *Rana esculenta* was studied under voltage clamp conditions. Mg^{2+} and La^{3+} reduce the sodium permeability, shift the voltage dependence of the Na permeability P_{Na} towards more positive potentials and reduce the effectiveness of TTX and STX. NO_3^- and SCN^- reduce the sodium permeability too, but shift the voltage dependence of P_{Na} towards more negative potentials and increase the action of TTX and STX. In all experiments the change in effectiveness is larger for the divalent STX than for the monovalent TTX. It is concluded that changes of the external surface potential induced by Mg^{2+}, La^{3+}, NO_3^- and SCN^- affect the TTX and STX binding to toxin receptors. The apparent potential change at the toxin receptor is only a fraction of the change 'seen' by the Na channel gates.

Key words: Frog node of Ranvier – Voltage clamp – TTX – STX – Surface charge

Introduction

The passive movement of Na ions through the sodium channel during excitation of nerve and muscle is reversibly inhibited by tetrodotoxin (TTX) and saxitoxin (STX). It appears that one TTX-molecule blocks one sodium channel (Hille 1968; Cuervo and Adelman 1970; Keynes et al. 1971; Colquhoun and Ritchie 1972a, b; Schwarz et al. 1973). Kao and Nishiyama (1965) suggested that the toxin molecule reaches – with its positively charged guanidinium group – into the channel and plugs it. Recent measurements led Kao to criticize his plug-in-the channel model (Kao and Walker 1982). He now proposes that TTX and STX bind to a receptor on the outer surface of the membrane, close to, but not inside the channel. The active guanidinium group is thought to be electrostatically attracted by fixed anionic charges around the orifice of the sodium channel, obstructing the latter, either in part or in whole, like a lid.

Radioactive TTX binds less well at low pH (Colquhoun et al. 1972; Benzer and Raftery 1972; Henderson and Wang 1972; Reed and Raftery 1976) and in the presence of monovalent cations like Li^+ and Tl^+, divalent cations and La^{3+} (Henderson et al. 1973, 1974). STX binding to rat muscles and rat heart is also inhibited by monovalent and divalent cations (Barchi and Weigele 1979; Lombet et al. 1981). Based on electrophysiological experiments, Hille (1971) proposed a 'selectivity filter' of the Na channel that includes an oxygen acid group at the proton binding site and could function as a receptor for binding TTX in a blocking position. Ulbricht and Wagner (1975) confirmed the idea that protons compete with the TTX-ion for the same site. The occupation of this site either by protons or by TTX would close the channel. In a short publication Hille et al. (1975a) investigated the influence of 20 mM Ca^{2+} on the effect of TTX and STX. They could explain their results best not by competition between calcium and toxin, but by the reduction of the negative surface potential by 20 mM Ca^{2+}.

In the present paper the influence of various cations and anions on the toxin action is investigated. The findings are compatible with the idea that the effective toxin concentration is determined by the negative surface potential near the binding site. Some of the results have been reported in a preliminary communication (Grissmer 1983).

Materials and methods

The experiments were carried out on single myelinated nerve fibres isolated from the N. ischiadicus of the frog *Rana esculenta*. Membrane currents were recorded under voltage clamp conditions at 15° C (Nonner 1969). The node under investigation was superfused continuously with Ringer's solution, containing 110 mM NaCl, 2.5 mM KCl, 1.8 mM $CaCl_2$, 5 mM Tris HCl buffer, pH 7.1–7.3. Potassium channels were blocked by 12 mM tetraethylammoniumchloride (TEA) present in all solutions. The Ag/AgCl electrodes were connected to the different pools of the perspex chamber with isotonic CsCl agar (120 mM) and the ends of the fibre were cut in 120 mM CsCl + 5 mM NaCl. Mg^{2+}- and La^{3+}-Ringer was prepared by adding solid $MgCl_2$ or $LaCl_3$ to normal Ringer's solution. In NO_3^-- or SCN^--Ringer NaCl was replaced by $NaNO_3$ or NaSCN.

All tetrodotoxin (TTX) solutions were prepared from the same 1 mg sample (Sankyo/Calbiochem). The stock solution contained 3.1 μM TTX in normal Ringer's solution. All saxitoxin (STX) solutions were prepared from the same stock solution (gift from Professor J. M. Ritchie, Yale University, New Haven, CT) containing 2.7 μM STX in normal Ringer's solution.

At the beginning of each experiment, the holding potential was adjusted so that the peak sodium current was 70% of the maximum sodium current measured after a −40 mV prepulse of 50 ms duration ($h_\infty = 0.7$). For $h_\infty =$

0.7 the membrane potential can be assumed to equal the normal resting potential of −70 mV (see Frankenhaeuser 1959). Subsequently, the holding potential was shifted to −92 mV in order to remove inactivation of the Na system completely. It remained at −92 mV during the entire experiment.

The command voltage pulses were generated by a microcomputer (DEC LSI 11/23), which was also used for sampling the data at 10-μs intervals and for off-line analysis. All current records were filtered with a 10-kHz low-pass filter and stored on floppy discs. The pulse duration was 5 ms and the pulse interval 1−2 s. To correct for capacitative and leakage currents the current associated with a −50 mV pulse was multiplied by −1, suitably scaled and subtracted from the total current.

Absolute values for the membrane current were obtained by assuming a longitudinal axoplasm resistance of 10 MΩ. Peak I_{Na} was converted to peak sodium permeability by means of the constant field equation (Goldman 1943; Hodgkin and Katz 1949)

$$P_{Na} = I_{Na} \frac{RT}{F^2 E} \frac{1}{[Na]_o} \frac{\exp(EF/RT) - 1}{\exp[(E - E_{Na})F/RT] - 1}. \quad (1)$$

$[Na]_o$ is the external Na concentration, E is the test pulse potential and E_{Na} is the Na equilibrium potential; F, R, and T have their usual meaning. To describe the voltage dependence of P_{Na}, peak P_{Na} (which is proportional to the square of the activation variable m) was fitted by a function related to the Boltzmann equation

$$P_{Na}(E) = \frac{\bar{P}_{Na}}{\{1 + \exp[(E_m - E)/k]\}^2} \quad (2)$$

where E_m is the potential at which $P_{Na} = 0.25\ \bar{P}_{Na}$ with $\bar{P}_{Na} = P_{Na_{max}}$ and k_m is a measure of the steepness of the curve (compare Dani et al. 1983). Shifts were calculated as the change of the midpoint potential E_m of the peak P_{Na} *(E)* curve. The same shifts and the same changes in toxin action were observed if P'_{Na} instead of peak P_{Na} was used; P'_{Na} was obtained by extrapolating the fast exponential decay of the sodium current back to zero time and represents the value which P_{Na} would attain if inactivation were to remain at its resting value (see Frankenhaeuser 1960).

The junction potential between the agar bridge (filled with 120 mM CsCl agar) in the A pool and the solution in the A pool was measured with a saturated KCl reference electrode at 15° C. The junction potential of NO_3^-- and SCN^--Ringer with respect to Ringer's solution was 0.5 mV and 1.0 mV (NO_3^-- and SCN^--Ringer negative). A small junction potential occurred in 1.08 mM La^{3+}- and 60 mM Mg^{2+}-Ringer (La^{3+}- and Mg^{2+}-Ringer 0.5 mV positive against normal Ringer); no measurable junction potential was observed with smaller La^{3+} or Mg^{2+} concentrations.

Reduction of I_{Na} reduces the voltage drop across the resistance in series with the membrane and thereby shifts the P_{Na} *(E)* curve by a few millivolt to more positive potentials (Drouin and Neumcke 1974). To correct for this effect, I measured the shifts occurring during TTX treatment in normal Ringer (e.g., a 3 mV shift accompanying a reduction of I_{Na} to 60%, see Figs. 1D and 2D) and subtracted an appropriately scaled value from the shifts observed in La^{3+}-, Mg^{2+}-, NO_3^--, and SCN^--Ringer.

The measured shifts of the P_{Na} *(E)* curve were not corrected for shifts due to the raised osmolality in solutions with added Mg^{2+} (compare Hille et al. 1975b).

Results

Reduction of the TTX-effect by di- and trivalent cations

The basic observation is illustrated in Fig. 1 which shows three I_{Na} *(E)* curves in the upper row (A−C) and the

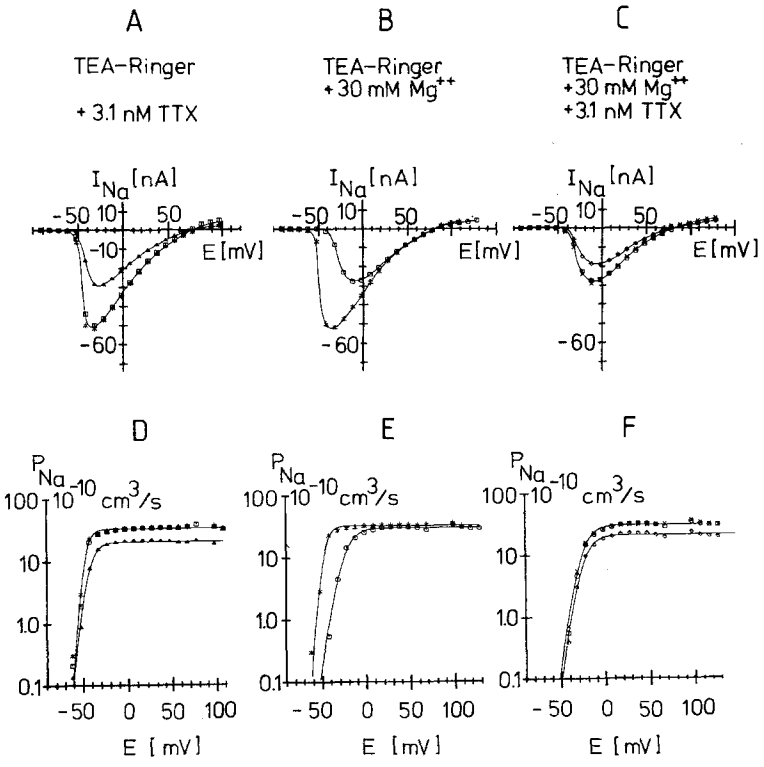

Fig. 1A−F. Effect of 3.1 nM TTX on peak I_{Na} and peak P_{Na} in the absence and in the presence of 30 mM Mg^{2+}. **A, D** Peak I_{Na} *(E)* and peak P_{Na} *(E)* in normal TEA-Ringer without TTX (□), with 3.1 nM TTX (△) and again without TTX (★). **B, E** Peak I_{Na} *(E)* and peak P_{Na} *(E)* in normal TEA-Ringer (★) and in TEA-Ringer with 30 mM Mg^{2+} (○). **C, F** Same as **A, D,** but in TEA-Ringer with 30 mM Mg^{2+}. All measurements were done on the same motor fibre 10 min after application of the respective solutions

Table 1. Modification of the TTX effect, shift of the ascending branch of the P_{Na} (E) curve and reduction of $\bar{P}_{Na}$ by various cations and anions. Columns (1) and (2) give $\bar{P}_{Na}$ in the presence of 3.1 nM TTX divided by $\bar{P}_{Na}$ in the absence of TTX for normal Ringer (control) and for test solution. Mean values ± SD. n = Number of experiments

Test solution	(1) Effect of 3.1 nM TTX control	(2) Effect of 3.1 nM TTX test solution	(3) Shift (mV)	(4) $\bar{P}_{Na}$ in (TTX-free) test solution divided by $\bar{P}_{Na}$ in (TTX-free) normal Ringer	n
0.135 mM La^{3+}	0.603 ± 0.016	0.644 ± 0.005	9.4 ± 1.1	0.897 ± 0.025	9
0.27 mM La^{3+}	0.603 ± 0.005	0.684 ± 0.006	16.1 ± 1.0	0.845 ± 0.033	7
0.54 mM La^{3+}	0.593 ± 0.011	0.701 ± 0.007	22.4 ± 0.7	0.728 ± 0.048	8
1.08 mM La^{3+}	0.616 ± 0.015	0.734 ± 0.008	30.2 ± 1.8	0.689 ± 0.033	6
10 mM Mg^{2+}	0.605 ± 0.005	0.651 ± 0.002	9.6 ± 0.7	0.908 ± 0.030	3
30 mM Mg^{2+}	0.606 ± 0.004	0.697 ± 0.002	20.0 ± 1.8	0.800 ± 0.034	7
60 mM Mg^{2+}	0.606 ± 0.003	0.720 ± 0.001	25.7 ± 1.6	0.781 ± 0.027	3
NO_3^-	0.608 ± 0.004	0.559 ± 0.005	−10.4 ± 1.4	0.923 ± 0.016	8
SCN^-	0.605 ± 0.003	0.516 ± 0.006	−19.7 ± 1.3	0.789 ± 0.053	5
Overall mean	0.605 ± 0.010				56

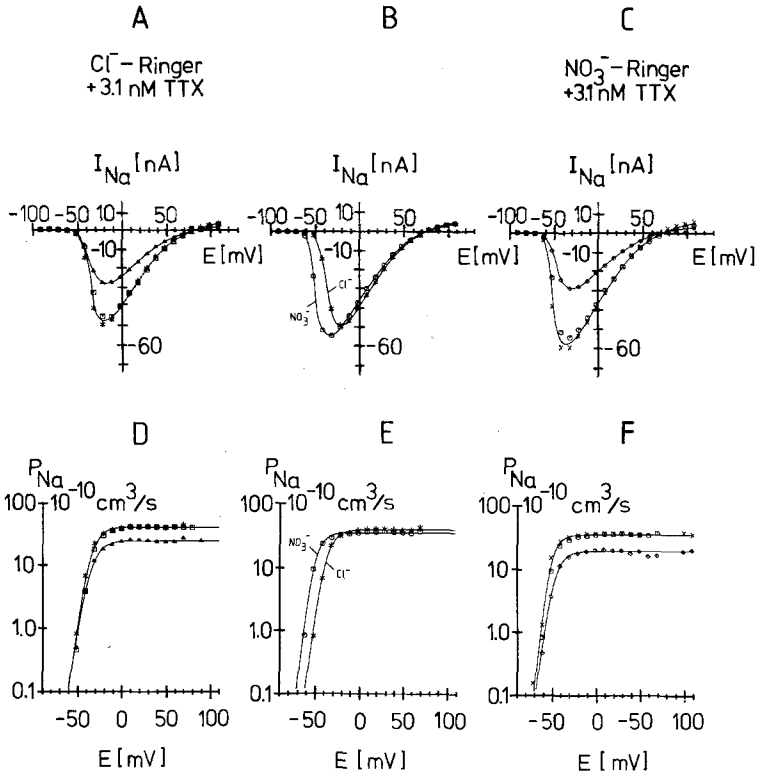

Fig. 2A–F. Effect of 3.1 nM TTX on peak I_{Na} and peak P_{Na} in Cl^--Ringer and in NO_3^--Ringer. **A, D** Peak I_{Na} (E) and peak P_{Na} (E) in normal Cl^--Ringer without TTX (□), with 3.1 nM TTX (△) and again without TTX (★). **B, E** Peak I_{Na} (E) and P_{Na} (E) in normal Cl^--Ringer (★) and in NO_3^--Ringer (○). **C, F** Same as **A, D,** but in NO_3^--Ringer. All measurements were done on the same motor fibre, 10 min after application of the respective solutions

corresponding P_{Na} (E) curves in the lower row (D–F). In normal Ringer (A, D,), 3.1 nM TTX reduced the Na inward current (measured at $E = 0$ mV) and the maximum Na permeability ($\bar{P}_{Na}$) to 61% of the control value; the effect was fully reversible. Addition of 30 mM Mg^{2+} to the Ringer solution (B, E) shifted the descending branch of the I_{Na} (E) curve and the ascending branch of the P_{Na} (E) curve to more positive values of membrane potential and decreased $\bar{P}_{Na}$ to 90%; the size of the shift was determined by measuring the change of the midpoint potential E_m of the P_{Na} (E) curve and (after subtraction of the series resistance artefact, see Methods) amounted to 20 mV. In Ringer with 30 mM Mg^{2+} (C, F), 3.1 nM TTX reduced I_{Na} and $\bar{P}_{Na}$ reversibly to 69%, i.e., the effect was slightly weaker than in normal Ringer.

The results of 56 experiments with different concentrations of Mg^{2+} and La^{3+} are summarized in Table 1. Comparing columns (1) and (2) shows that all solutions with La^{3+} or Mg^{2+} reduce the TTX effect. The reduction of the TTX effect was most pronounced in Ringer with 1.08 mM La^{3+}. This solution produced also the largest shift of the P_{Na} (E) curve (column 3) and the largest decrease of $\bar{P}_{Na}$ (column 4). The observed shifts and the decreases of $\bar{P}_{Na}$ agree well with the findings of Brismar (1980), whereas

Vogel (1974) described a larger shift and a larger decrease of $\bar{P}_{Na}$ in La^{3+}.

Increase of the TTX-effect by anions

In Fig. 2 the same kind of experiment as in Fig. 1 was done to test the effect on NO_3^--Ringer on the TTX action. In normal Cl^--Ringer (A, D) 3.1 nM TTX reduced the Na inward current (measured at $E = 0$ mV) and the maximum Na permeability ($\bar{P}_{Na}$) to 61% of the control value; the effect was fully reversible. Replacing the Cl^--Ringer by NO_3^--Ringer (B, E) shifted the descending branch of the I_{Na} *(E)* curve and the ascending branch of the P_{Na} *(E)* curve by 11 mV (after subtraction of the series resistance artefact and correction for junction potential, see Methods) to more negative values of membrane potential and decreased $\bar{P}_{Na}$ to 90%. In NO_3^--Ringer (C, F), 3.1 nM TTX reduced I_{Na} and $\bar{P}_{Na}$ reversibly to 55%, i.e., the effect of TTX was slightly stronger than in normal Cl^--Ringer.

The effect of TTX was more increased if SCN^- was used instead of NO_3^- as can be seen in Table 1. The shift of the P_{Na} *(E)* curve and the reduction of $\bar{P}_{Na}$ were also more pronounced in SCN^--Ringer. The shift of the ascending branch of the P_{Na} *(E)* curve and the reduction of $\bar{P}_{Na}$ by NO_3^- and SCN^- are in good agreement with the data in Table I and II of Dani et al. (1983).

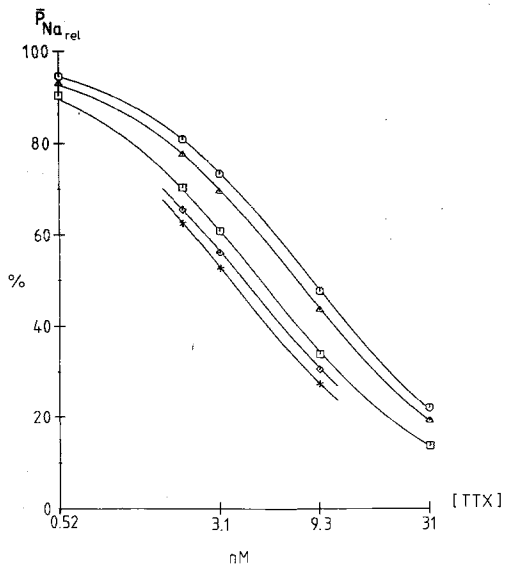

Fig. 3. Steady-state effect of TTX on $\bar{P}_{Na}$ in 1.08 mM La^{3+}-, 30 mM Mg^{2+}-, Cl^--, NO_3^-- and SCN^--Ringer. $\bar{P}_{Na_{rel}}$ is given in % of the respective values in the solutions without TTX. [TTX] is plotted on a logarithmic scale. The points are mean values obtained from at least three experiments. The points belonging to the control solution represent at least 15 experiments. The SD does not exceed the size of the symbols. The curves through the points were calculated assuming the relative $\bar{P}_{Na}$ to be proportional to $K_D/([TTX] + K_D)$. Numerical values for K_D are given in column (1) of Table 2. ○ La^{3+}, △ Mg^{2+}; □ Cl^- (control); ◇ NO_3^-; ★ SCN^-

Dose response curves

In further experiments, several TTX concentrations were tested in each solution in order to construct dose-response curves. Figure 3 shows the relative $\bar{P}_{Na}$ as a function of TTX concentration [TTX] in solutions with different cations and anions. The curves through the points were calculated assuming the relative $\bar{P}_{Na}$ to be proportional to $K_D/([TTX] + K_D)$ where K_D is the equilibrium dissociation constant (see Schwarz et al. 1973). The K_D value of the TTX reaction in normal Ringer solution was 4.79 nM and is somewhat larger than the value of 3.6 nM given by Schwarz et al. (1973). 1.08 mM La^{3+} and 30 mM Mg^{2+} increased the K_D value to 8.5 nM and 7.1 nM, respectively, whereas NO_3^-- and SCN^--Ringer decreased K_D to 3.9 nM and 3.3 nM, respectively.

Change of the STX effect by cations and anions

As pointed out by Hille et al. (1975a), changes in surface potential should affect the divalent STX more strongly than the monovalent TTX. Therefore, I compared the effect of the various cations and anions on the TTX block with their effect on the STX block.

Figure 4 shows the effect of 1.35 nM STX in Cl^--Ringer and in SCN^--Ringer. In Cl^--Ringer the peak Na inward current is reduced to 49% whereas the reduction in SCN^--Ringer is to 32%. Thus, SCN^--Ringer markedly enhances the STX block; the enhancement of the STX Block is more pronounced than the enhancement of the TTX block (see Table 1). In similar experiments the effect

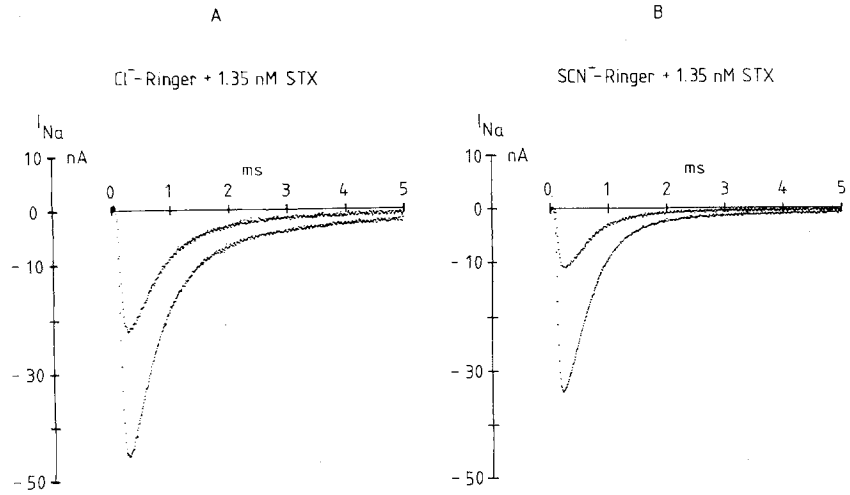

Fig. 4A, B. Effect of STX on the sodium inward current I_{Na} in Cl^--Ringer and in SCN^--Ringer. Na inward current associated with a 5-ms pulse to −2 mV in Cl^--Ringer with and without 1.35 nM STX **(A)** and in SCN^--Ringer with and without 1.35 nM STX **(B).** All measurements were done on the same motor fibre, 15 min after application of the respective solutions

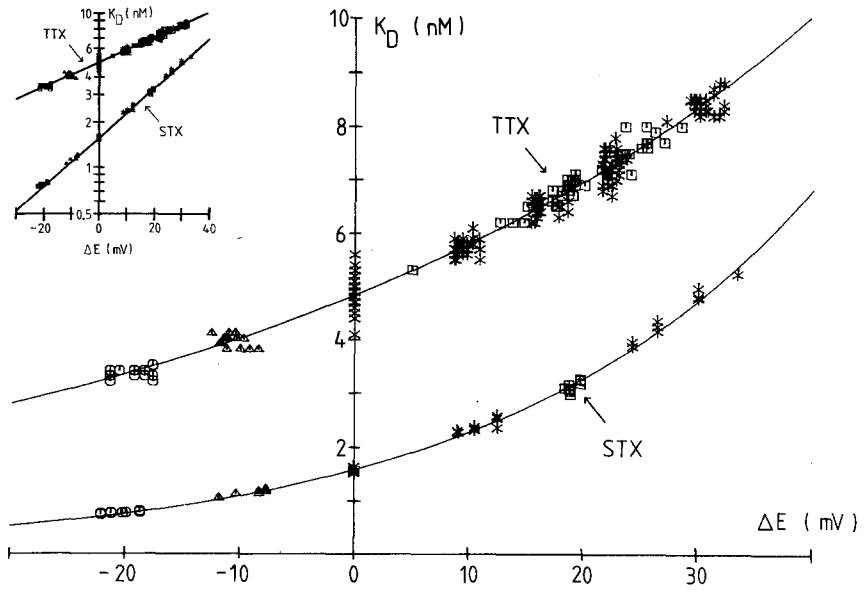

Fig. 5. Equilibrium dissociation constant K_D for TTX and *STX* plotted against the voltage shift ΔE. K_D values calculated from the relative $\bar{P}_{Na}$ as in column (1) of Table 2. ΔE determined from the shift of the ascending branch of the P_{Na} *(E)* curve. Measurements in normal Ringer (×), in Ringer with La^{3+} (★) or Mg^{2+} (□), in NO_3^--Ringer (△) and in SCN^--Ringer (○). Points for *TTX* fitted by the equation $K_D = 4.81 \exp(18.41\ 10^{-3}\ \Delta E)$ [nM] with ΔE in millivolt. Curve for STX calculated from the equation $K_D = 1.56 \exp(36.82\ 10^{-3}\ \Delta E)$ [nM]. *Inset:* K_D versus ΔE replotted with K_D on a logarithmic scale to illustrate more clearly the different slopes of the two curves

of 0.135 mM La^{3+}-, 1.08 mM La^{3+}-, 30 mM Mg^{2+}-, and NO_3^--Ringer on the block produced by 0.54 nM, 1.35 nM, and 3.375 nM STX was studied. K_D values for STX were calculated from the relative $\bar{P}_{Na}$ values as in the experiments with TTX. In normal Ringer the K_D was 1.56 ± 0.03 nM (mean ± SD from 29 measurements), which is in reasonable agreement with the value of 1.4 nM given by Wagner and Ulbricht (1975) and Barchi and Weigele (1979).

In Fig. 5, the K_D values for TTX and STX measured in the various solutions are plotted against the shifts ΔE of the P_{Na} *(E)* curve obtained in the same solutions. The curve through the points for TTX was fittet with the help of an exponential function. It intersects the ordinate axis at 4.81 nM; this agrees well with the K_D value of 4.79 nM in normal Ringer solution. From the slope of the curve one can calculate that the TTX receptor sees only 46% (= 0.0184 × *RT/F*) of the negative surface potential seen by the gating machinery (*m*-gates). A curve with a two times larger slope (to account for the two positive charges of the STX molecule) was drawn through the point $K_D = 1.56$ nM at $\Delta E = 0$ mV. It clearly provides a good fit to the points measured with STX. (No satisfactory fit was obtained with a 1.5 times larger slope; in this case the calculated K_D at $\Delta E = 30$ mV was 3.6 nM which is significantly smaller than the measured K_D values). The larger slope of the STX curve is best seen when K_D is plotted on a logarithmic scale (see inset of Fig. 5). It indicates that ΔE affects the action of STX more strongly than the action of TTX. For example, changing ΔE from 0 to 20 mV increases the K_D value for STX by a factor of 2.1 and the K_D value for TTX by a factor of only 1.44.

Discussion

Earlier investigators found a reduction of the TTX and STX effect by Ca^{2+} (Hille et al. 1975a) and a reduction of the TTX effect by H^+ (Ulbricht and Wagner 1975). The present paper shows that Mg^{2+} and La^{3+} too reduce the TTX and STX effect, whereas NO_3^- and SCN^- increase the effect of the two toxins.

The most likely explanation is that the observed changes are caused by changes in the effective TTX or STX concentration due to changes of the surface potential in the vicinity of the toxin binding site. As shown by Fig. 5, the K_D values for TTX and STX measured in the various solutions are correlated to the voltage shifts of the P_{Na} *(E)* curve that occur in these solutions. The changes in K_D are apparent changes. They can be quantitatively explained by assuming that the toxin receptor sees only 46% of the voltage shift ΔE seen by the *m*-gates. In this case the effective TTX concentration at the toxin receptor equals $[TTX] \cdot \exp(-0.46\ \Delta E \cdot F/RT)$ and K_D values are almost constant [see column (4) of Table 2].

An alternative assumption would be that the divalent or trivalent cations compete with TTX or STX for the same receptor whose occupation results in the occlusion of the channel. In this case the fraction of channels blocked by TTX will be

$$1 - p_T' = \frac{c_{TTX}}{c_{TTX} + c_{cat} + 1} \qquad (3)$$

where c_{TTX} and c_{cat} are the normalized concentrations of TTX and competing cations defined by $c_{TTX} = [TTX]/K_D$ and $c_{cat} = [\text{cations}]/K_{D_{cat}}$ (see Ulbricht and Wagner 1975). Solving for c_{TTX} and substituting the expression for c_{TTX} into the equation $K_D = [TTX]/c_{TTX}$ leads to a new equation for K_D (see footnote [c] in Table 2). K_D values calculated from this equation [see column (2) of Table 2] increase with increasing concentration of La^{3+} and Mg^{2+}, a finding that argues against simple competition. This difficulty could be removed by a mixed model assuming competition plus a surface potential-induced change of the effective toxin concentration (assuming for instance that the TTX receptor experiences 24% of the negative surface potential seen by the gating machinery): in this case the K_D values become independent of the La^{3+} or Mg^{2+} concentration [column (3) of Table 2]. The competition model fails, however, to explain the increase of TTX-sensitivity in NO_3^-- and SCN^--Ringer.

Strong support for the surface potential hypothesis comes from the observation that the effect of the divalent

Table 2. Apparent equilibrium dissociation constant, K_D, of TTX site reaction as calculated for the case of (1) exclusive change of 'affinity' of the toxin receptor in a two-site situation, (2) competition, (3) competition plus surface potential-induced change of effective toxin concentration, and (4) surface potential effect alone. The equations used are from Ulbricht and Wagner (1975) and given below

Test solution	c_{cat}[a]	n	K_D calculated for assumptions			
			(1)[b] nM	(2)[c] nM	(3)[d] nM	(4)[e] nM
Control	0	107	4.79	4.79	4.79	4.79
0.135 mM La^{3+}	0.115	26	5.75	5.16	4.69	4.81
0.27 mM La^{3+}	0.183	23	6.58	5.56	4.73	4.85
0.54 mM La^{3+}	0.374	28	7.39	5.37	4.28	4.83
1.08 mM La^{3+}	0.451	18	8.50	5.86	4.36	4.89
10 mM Mg^{2+}	0.101	3	5.79	5.26	4.76	4.80
15 mM Mg^{2+}	0.101	3	6.21	5.64	4.93	4.82
20 mM Mg^{2+}	0.151	5	6.48	5.63	4.79	4.78
25 mM Mg^{2+}	0.167	3	6.78	5.81	4.85	4.83
30 mM Mg^{2+}	0.250	19	7.11	5.69	4.65	4.88
35 mM Mg^{2+}	0.236	3	7.23	5.85	4.67	4.75
40 mM Mg^{2+}	0.229	3	7.43	6.05	4.81	4.84
50 mM Mg^{2+}	0.285	3	7.68	5.98	4.65	4.79
60 mM Mg^{2+}	0.364	3	7.93	5.81	4.49	4.89
NO_3^-		14	3.95			4.77
SCN^-		12	3.33			4.81

[a] $c_{cat} = \frac{1-\alpha}{\alpha}$; $\alpha = \frac{\bar{P}_{Na} \text{ of test solution}}{\bar{P}_{Na} \text{ of control solution}}$

[b] $K_D = [TTX]/(1/p_T' - 1)$; $p_T' = \frac{\bar{P}_{Na} \text{ of test solution + TTX}}{\bar{P}_{Na} \text{ of test solution}}$

[c] $K_D = [TTX]/(1/p_T' - 1) \cdot (c_{cat} + 1)$

[d] $K_D = \{[TTX]/(1/p_T' - 1) \cdot (c_{cat} + 1)\} \exp \cdot (-0.24\, \Delta E \cdot F/RT)$

[e] $K_D = \{[TTX]/(1/p_T' - 1)\} \exp \cdot (-0.46\, \Delta E \cdot F/RT)$

STX is more affected by Mg^{2+}, La^{3+}, NO_3^-, and SCN^- than the effect of the monovalent TTX. This finding confirms and extends the observation of Hille et al. (1975a) that increasing the Ca^{2+} concentration from 2 to 20 mM reduces the effectiveness of STX more than that of TTX. They could explain their results with both toxins by a change in surface potential of 7.2–7.6 mV, a potential change which is only 30% of that seen by the *m*-gates. Figure 5 of the present paper shows that the change of K_D with ΔE observed with STX can be predicted from the K_D (ΔE) curve measured with TTX if allowance is made for the different valencies of the two toxins. Similarly, Ritchie and Rogart (1977) were able to predict quantitatively the effect of Ca^{2+} on TTX binding from measurements of STX binding in different Ca^{2+} concentrations, taking into account that TTX is monovalent and STX divalent (see their Fig. 9). The agreement between predicted and measured values in Fig. 5 of the present paper and in Fig. 9 of Ritchie and Rogart (1977) is surprising because in both cases the complications arising from the finite size of the STX^{2+} cation (see Carnie and McLaughlin 1983; Alvarez et al. 1983) have been ignored.

The idea that the surface potential affects the toxin binding site is further supported by the finding that substitution of NO_3^- or SCN^- for Cl^- (which increases the negative surface potential) increases the effectiveness of TTX and STX. There are numerous studies describing the effect of foreign anions on the electrical excitability of nerve and muscle (for review, see Horowicz 1964; and Dani et al. 1983), but, to my knowledge, no publications concerning the influence of anions on drug effects [apart from a brief statement in Henderson et al. (1973) that substitution of NO_3^- for Cl^- has no effect on STX binding]. Only recently, Neumcke and Stämpfli (1984) in noise measurements on the node of Ranvier determined the number of conducting Na channels in Cl^-- and NO_3^--Ringer with 8 nM TTX. In contrast to my results, they did not observe an enhancement of the TTX effect in NO_3^--Ringer. They found, however, an increase of the STX effect in SCN^--Ringer (Neumcke and Stämpfli, personal communication).

Finally, it should be pointed out that the calculation of K_D values from measurements of I_{Na} or $\bar{P}_{Na}$ is based on the assumption that TTX and STX merely reduce the number of conducting channels (N) but do not alter the single channel conductance (γ). Earlier noise measurements supported this assumption (Sigworth 1980) but a more recent investigation showed an increase of γ after application of 8 nM TTX (Neumcke and Stämpfli 1983). Because of the increase in γ, K_D values deduced from measurements of I_{Na} or $\bar{P}_{Na}$ are larger than the (real) K_D values determined from measurements of N (see Neumcke and Stämpfli 1983). Likewise the changes of K_D produced by the various cations and anions are larger for K_D calculated from I_{Na} or $\bar{P}_{Na}$ than for K_D calculated from N. Consequently, the fraction of the electric field seen by the toxin binding site may actually be smaller than the value of 0.46 given above.

Acknowledgements. The author is greatly indebted to Professor Hans Meves for his helpful advice and discussion, to Professor B. Neumcke and Professor W. Ulbricht for reading and commenting on the manuscript, to Professor J. M. Ritchie for kindly providing

saxitoxin and to Mrs. R. Stolz for typing the manuscript. This work was supported by the Deutsche Forschungsgemeinschaft, SFB 38 "Membranforschung".

References

Alvarez O, Brodwick M, Latorre R, McLaughlin A, McLaughlin S, Szabo G (1983) Large divalent cations and electrostatic potentials adjacent to membranes. Experimental results with hexamethonium. Biophys J 44: 333–342

Barchi RL, Weigele JB (1979) Characteristics of saxitoxin binding to the sodium channel of sarcolemma isolated from rat skeletal muscle. J Physiol 295: 383–396

Benzer TI, Raftery MA (1972) Partial characterisation of a tetrodotoxin-binding component from nerve membrane. Proc Natl Acad Sci USA 69: 3634–3637

Brismar T (1980) The effect of divalent and trivalent cations on the sodium permeability of myelinated nerve fibres of *Xenopus laevis*. Acta Physiol Scand 108: 23–29

Carnie S, McLaughlin S (1983) Large divalent cations and electrostatic potentials adjacent to membranes. A theoretical calculation. Biophys J 44: 325–332

Colquhoun D, Ritchie JM (1972a) The interaction at equilibrium between tetrodotoxin and mammalian non-myelinated nerve fibres. J Physiol 221: 533–553

Colquhoun D, Ritchie JM (1972b) The kinetics of the interaction between tetrodotoxin and mammalian non-myelinated nerve fibres. Molec Pharmacol 8: 285–292

Colquhoun D, Henderson R, Ritchie JM (1972) The binding of labelled tetrodotoxin to non-myelinated nerve fibres. J Physiol 227: 95–126

Cuervo LA, Adelman WJ (1970) Equilibrium and kinetic properties of the interaction between tetrodotoxin and the excitable membrane of the squid giant axon. J Gen Physiol 55: 309–335

Dani JA, Sanchez JA, Hille B (1983) Lyotropic anions. Na channel gating and Ca electrode response. J Gen Physiol 81: 255–281

Drouin H, Neumcke B (1974) Specific and unspecific charges at the sodium channels of the nerve membrane. Pflügers Arch 351: 207–229

Frankenhaueser B (1959) Steady state inactivation of sodium permeability in myelinated nerve fibres of *Xenopus laevis*. J Physiol 148: 671–676

Frankenhaeuser B (1960) Quantitative description of sodium currents in myelinated nerve fibres of *Xenopus laevis*. J Physiol 141: 491–501

Goldman DE (1943) Potential, impedance, and rectification in membranes. J Gen Physiol 27: 37–60

Grissmer S (1983) Influence of Ca, Mg, La on equilibrium effects of tetrodotoxin on myelinated frog nerve fibres. Naunyn-Schmiedeberg's Arch Pharmacol 322: R66

Henderson R, Wang JH (1972) Solubilization of a specific tetrodotoxin-binding component from garfish olfactory nerve membrane. Biochemistry 11: 4565–4569

Henderson R, Ritchie JM, Strichartz GR (1973) The binding of labelled saxitoxin to the sodium channels in nerve membranes. J Physiol 235: 783–804

Henderson R, Ritchie JM, Strichartz GR (1974) Evidence that tetrodotoxin and saxitoxin act at a metal cation binding site in the sodium channels of nerve membrane. Proc Natl Acad Sci USA 71: 3936–3940

Hille B (1968) Pharmacological modifications of the sodium channels of the frog nerve. J Gen Physiol 51: 199–219

Hille B (1971) The permeability of the sodium channel to organic cations in myelinated nerve. J Gen Physiol 58: 599–619

Hille B, Ritchie JM, Strichartz GR (1975a) The effect of surface charge on the nerve membrane on the action of tetrodotoxin and saxitoxin in frog myelinated nerve. J Physiol 250: 34–35P

Hille B, Woodhull AM, Shapiro BJ (1975b) Negative surface charge near sodium channels of nerve: divalent ions, monovalent ions, and pH. Phil Trans R Soc Lond B 270: 301–318

Hodgkin AL, Katz B (1949) The effect of sodium ions on the electrical activity of the giant axon of the squid. J Physiol 108: 37–77

Horowicz P (1964) The effects of anions on excitable cells. Pharmacol Rev 16: 193–221

Kao CY, Nishiyama A (1965) Actions of saxitoxin on peripheral neuromuscular systems. J Physiol 180: 50–66

Kao CY, Walker SE (1982) Active groups of saxitoxin and tetrodotoxin as deduced from actions and saxitoxin analogues on frog muscle and squid axon. J Physiol 323: 619–637

Keynes RD, Ritchie JM, Rojas E (1971) The binding of tetrodotoxin to nerve membranes. J Physiol 213: 235–254

Lombet A, Renaud JF, Chicheportiche R, Lazdunski M (1981) A cardiac tetrodotoxin binding component: Biochemical identification, characterization and properties. Biochemistry 20: 1279–1285

Neumcke B, Stämpfli R (1983) Alteration of the conductance of Na^+ channels in the nodal membrane of frog nerve by holding potential and tetrodotoxin. Biochim Biophys Acta 727: 177–184

Neumcke B, Stämpfli R (1984) Heterogeneity of external surface charges near sodium channels in the nodal membrane of frog nerve. Pflügers Arch 401: 125–131

Nonner W (1969) A new voltage clamp method for Ranvier nodes. Pflügers Arch 309: 176–192

Reed JK, Raftery MA (1976) Properties of the tetrodotoxin binding component in plasma membranes isolated from *Electrophorus electricus*. Biochemistry 15: 944–953

Ritchie JM, Rogart RB (1977) The binding of saxitoxin and tetrodotoxin to excitable tissue. Rev Physiol Biochem Pharmacol 79: 1–50

Schwarz JR, Ulbricht W, Wagner HH (1973) The rate of action of tetrodotoxin in myelinated nerve fibres of *Xenopus laevis* and *Rana esculenta*. J Physiol 233: 167–194

Sigworth FJ (1980) The conductance of sodium channels under conditions of reduced current at the node of Ranvier. J Physiol 307: 131–142

Ulbricht W, Wagner HH (1975) The influence of pH on equilibrium effects of tetrodotoxin on myelinated nerve fibres of *Rana esculenta*. J Physiol 252: 159–184

Vogel W (1974) Calcium and lanthanum effects at the nodal membrane. Pflügers Arch 350: 25–39

Wagner HH, Ulbricht W (1975) The rates of saxitoxin action and of saxitoxin-tetrodotoxin interaction at the node of Ranvier. Pflügers Arch 359: 297–315

Received May 19/Accepted July 27, 1984